

Digital Pulse-Shape Analyzer Based on Fast Sampling of an Integrated Charge Pulse

Valentin T. Jordanov* and Glenn F. Knoll

The University of Michigan, Dept. of Nuclear Engineering, Ann Arbor, MI. 48109

Abstract

A novel configuration for pulse-shape analysis and discrimination has been developed. The current pulse from the detector is sent to a gated integrator and then sampled by a flash analog-to-digital converter (ADC). The sampled data are processed digitally, thus allowing implementation of a near-optimum weighting function and elimination some of the instabilities associated with the gated integrator. The analyzer incorporates pileup rejection circuit that reduces the pileup effects at high counting rates. The system was tested using a liquid scintillator. Figures of merit for neutron-gamma pulse-shape discrimination were found to be: 0.78 for 25 keV (electron equivalent energy) and 3.5 for 500 keV.

I. INTRODUCTION

One of the most commonly used techniques for pulse-shape discrimination (PSD) is the charge comparison method [1, 2]. This method is based on a simple weighting function [3] which limits the separation ability of the discriminator at low energies.

The technique described in this paper was developed to be used in a near tissue-equivalent neutron-gamma dosimeter which employs a liquid scintillator detector. The accuracy of the dosimeter depends on the ability of the pulse-shape analyzer to separate gamma spectrum from neutron pulse-height distribution. Our objective was to improve the PSD at low energies by implementing near optimum filter for processing the detector signal.

II. OPTIMAL WEIGHTING FUNCTION FOR PULSE-SHAPE DISCRIMINATION

Consider a pulse-shape analyzer based on a single gated integrator and a fast sampling ADC. The gated integrator signal is sampled many times in equal periods of time synchronized with the beginning of the detector signal. The digital samples are then processed by a linear filter given as

$$s = \sum_{i=1}^n W_i \cdot g_i \quad (1)$$

where g_i is the sampled signal, W_i are the filter weights and n is the total number of samples including the last sample which represents the total charge. Hence, a ratio which characterizes the pulse shape is given by

$$r = \frac{s}{g_n} = \frac{\sum_{i=1}^{n-1} W_i \cdot g_i}{g_n} + W_n \quad (2)$$

where the weight W_n only causes an offset in the ratio spectrum and can be omitted. Note that the charge comparison method is a particular case of the filter defined in Eqn 1. In this case there is only one non-zero weight: the one that corresponds to the fast charge component.

The ratio signal is subject to uncertainties due to statistical fluctuations of the detector signal. Therefore, the effective separation of two or more pulse shapes is sensitive to the weighting function of the filter defined in Eqn 1.

The optimal weighting function for pulse-shape discrimination has been derived by Gatti and De Martini [4]. In this work a linear filter for processing current pulses from photomultiplier anode is considered. The response of the filter can be expressed as

$$s = \sum_{i=1}^n P_i \cdot v_i \quad (3)$$

where v_i is sampled current signal and P_i are filter weights.

Gatti describes the current pulses as a succession of the number of electrons emitted in equal time intervals. Following Gatti's notation, these quantities of charges for two pulses with different shapes, $\alpha(t)$ and $\gamma(t)$, are α_i and γ_i respectively, where i is the time interval of charges α_i and γ_i . The difference between the two weighted signals is given by

$$\Delta = \sum_{i=1}^n P_i (\alpha_i - \gamma_i) \quad (4)$$

where P_i are the desired weights.

The weights P_i are found from the condition for minimization of the relative variance of Δ in Eqn 4. The optimum weights are [4]

$$P_i = \frac{\alpha_i - \gamma_i}{\alpha_i + \gamma_i} \quad (5)$$

Equation 5 does not account for uncertainties due to the dark current of the photomultiplier and to the effects of pileup. A modified expression for the optimal weights was derived also by De Martini and Gatti [5]. With the introduction of bi-alkali photocathodes, thermionic noise has become an insignificant factor in PSD using small diameter photomultiplier tubes. The effect of pileup can be effectively eliminated by using pileup rejection techniques. Therefore, the weights defined by Eqn 5 are chosen as optimal in the following discussion.

* Present address: Amptek, Inc., 6 De Angelo Dr., Bedford, MA. 01730.

The filter defined by Eqn 3 can be realized by direct sampling of the detector current pulse. Sampling fast pulses (fast rise time) requires the use of wide bandwidth fast ADCs [6], whose amplitude resolution is currently limited to 8 bits. It is also necessary to precisely measure the total charge which for fast pulses can be done by using an analog gated integrator. Thus, to allow the use of higher digital resolution, and to accurately measure the total charge, a system was developed which is based on a single gated integrator followed by a fast sampling ADC.

Consider the case where the total number of samples per measurement of a single event is n . The integrated signal can be expressed as function of the sampled current signal v_i

$$g_i = \sum_{k=1}^i v_k \quad (6)$$

For optimal pulse-shape discrimination the response of the gated integrator system must be the same as the response of the filter defined by Eqn 3. In other words, the weights W_i must satisfy the following equation

$$s = \sum_{i=1}^n P_i v_i = \sum_{i=1}^n W_i g_i \quad (7)$$

To obtain W_i we first express v_i in terms of g_i

$$v_i = g_i - g_{i-1} \quad 2 \leq i \leq n \quad (8)$$

Substituting Eqn 8 into Eqn 7 gives

$$s = P_1 g_1 + P_2 (g_2 - g_1) + \dots + P_n (g_n - g_{n-1}) \quad (9)$$

Eqn 9 can be rewritten as

$$s = (P_1 - P_2)g_1 + (P_2 - P_3)g_2 + \dots + (P_{n-1} - P_n)g_{n-1} + P_n g_n \quad (10)$$

Hence, the solution for W_i is

$$W_i = P_i - P_{i+1} \quad 1 \leq i \leq n-1 \quad (11)$$

Using Equations 5, 8 and 11, the weights W_i can be obtained for the sampled gated integrator signal. The procedure for determining W_i is as follows. First, pulse shapes corresponding to two different particles are recorded separately. Second, both pulse shapes are normalized to the same total charge (the last sample of the integrated signal). Third, Equations 5 and 8 are used to calculate the weights P_i . Finally, the weights W_i are determined from Eqn 11. In the next section we describe a pulse shape analyzer that allows particle identification based on the algorithm given by Eqn 2.

III. DIGITAL PULSE-SHAPE ANALYZER

The block diagram of the digital pulse-shape analyzer is shown in Fig. 1. The anode current from the photomultiplier produces a voltage pulse across a load resistor (R_L). This voltage pulse passes through a fanout buffer (BUF). Two branches are fed by the buffered signal. In the first branch a constant-fraction discriminator (CFD) is used to generate a timing strobe that indicates the beginning of the detector pulse. The signal in the second branch is used to stabilize the DC level through the baseline stabilizer (DCS). This signal

is also applied via a delay line (DELAY1) to the input of the gated integrator. The gated integrator is switched by a gate signal from the output of a D-trigger (DT1). This trigger is activated by the timing signal from CFD. The gate signal also enables a gated clock generator so that a flash ADC (AD9020, 10 bit, 50MHz) begins sampling the output of the gated integrator. Note that the sampling clock and the occurrence of the detector pulses are synchronized. The delay time of DELAY1 is set to be longer than two sampling periods plus the time required to switch the gated integrator. During this delay time the DC offset at the output of the gated integrator is measured. This offset (known as a pedestal) is due to charge injection to the gated integrator input through the analog switch. The pedestal is estimated using the first two samples in each pulse measurement sequence. For each event the average of these two samples is subtracted from the rest of the event samples. This correction also accounts for any possible drift (temperature, aging, power fluctuations) of the baseline of the circuits following the gated integrator.

The gated clock is also applied to a first-in-first-out register (FIFO) where the signal samples are stored in queue fashion. At the beginning of the gate signal, a digital number corresponding to the maximum number of samples per event is loaded into a binary down-counter. After the gated clock is enabled, the content of the down counter decrements until it reaches zero. At this point a reset signal is generated which returns the circuit to the initial state. In order to distinguish between events, an event recognition signal (ERF) is generated by the trigger (TT). This one-bit signal toggles between one and zero each time a new event is recorded. For samples from a given event, this bit remains in a given state, changing only when a record of a new event begins.

Pileup rejection is another function implemented in this circuit. At high counting rates, pileup causes erroneous recording of pulse-shape information. A second D-trigger (DT2) is used to discriminate between single and pileup events. Initially, before processing a new detector pulse, DT1 and DT2 are set to zero. A master-slave configuration is used in which DT1 is the master trigger while DT2 is the slave. The first pulse from CFD causes DT1 to change its output state to one. At the same time, DT2 follows the previous state of DT1, which was zero. If there is a second pulse from CFD during the gate signal, the state at the output of DT2 changes from zero to one. The signal from DT2 passes through a delay line (DELAY2) and is stored in FIFO as a pileup flag (PUF). The second delay is set to be the same as the delay of the signal in the gated integrator branch for synchronization purposes. If there is no pileup event during the gate period the flag PUF, remains zero. Signal oscillograms at the major points of the circuit are shown in Fig. 2.

The data from FIFO are read by a personal computer (Intel486 processor, 66 MHz). The processing algorithm was implemented in software written in C and Assembly languages. The assembly routine allows a maximum recording rate of 10,000 events per second, while the limit imposed by the C routine is 5,000 events per second. Higher

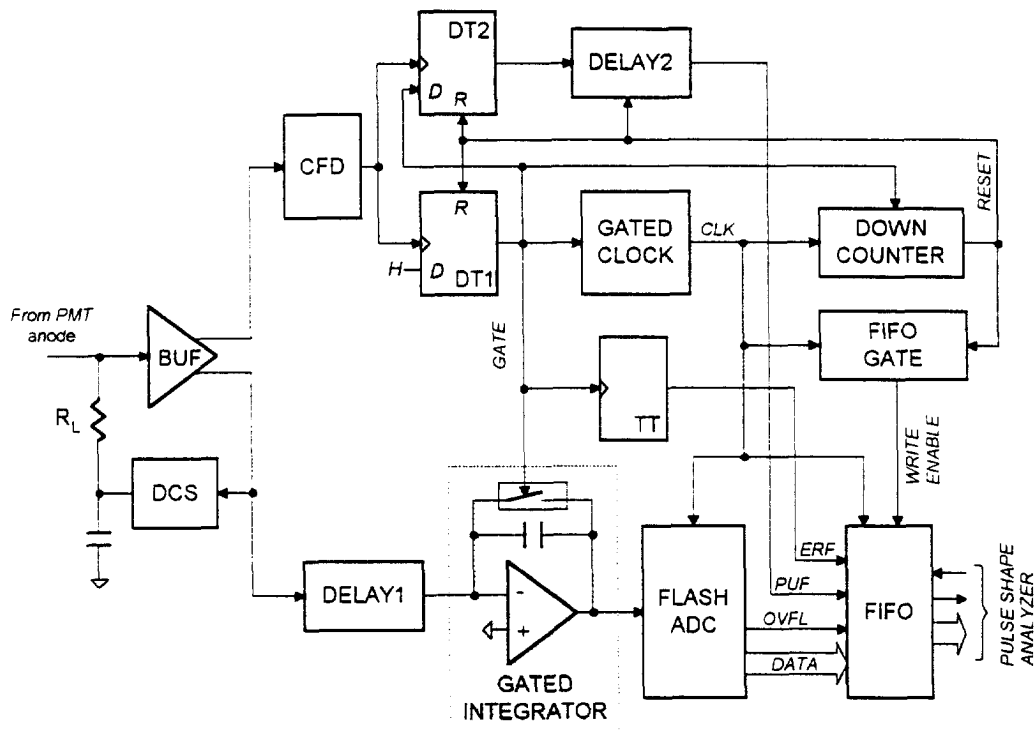


Fig. 1 Block diagram of the digital pulse-shape analyzer.

processing rates can be achieved using digital signal processors or a dedicated hardware circuit.

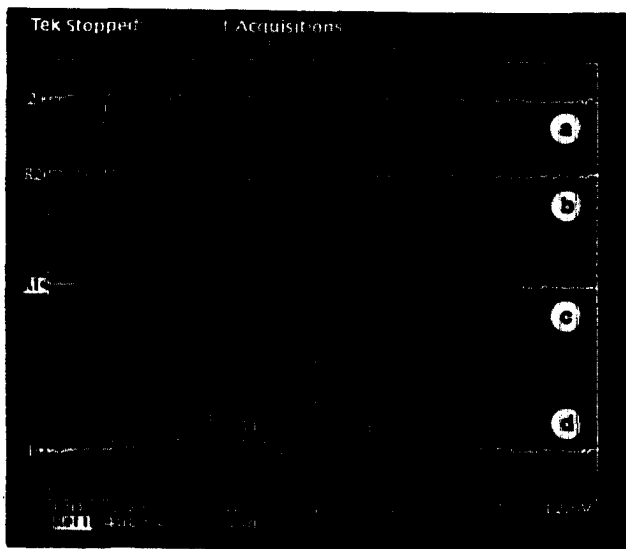


Fig. 2 Oscilloscope signals at: output of the constant fraction discriminator (a), output of the delay line 1 (b), inverted output of the gated integrator (c), and the synchronized sampling clock (d).

IV. EXPERIMENTAL MEASUREMENTS

The digital pulse-shape analyzer was used for pulse-shape discrimination between neutron and gamma pulses from a liquid scintillator. The detector is constructed in the form of

a right circular cylinder (38x38 mm) filled with liquid scintillator BC501A (Bicron). This cell is coupled to an R980 photomultiplier tube (Hamamatsu) with a very low anode dark current (less than 3.5 nA). A 1 Ci Pu-Be neutron source was placed adjacent to the detector. The counting rate from the CFD was 50,000 counts per second. The full range of the ADC corresponds to approximately 500 keV energy deposited by gamma interactions. This energy is often termed *electron equivalent energy* (measured in keV_{ee} or MeV_{ee}).

First the weighting function for optimal separation of the pulses produced by gamma and neutron interactions was found. A software routine was written for calculating the ratios and separation of neutron and gamma pulses. This routine also performs rejection of pileup and overflow events using the information provided by the corresponding flags (see description of the hardware). At the very early stage of determining the optimal weighting function, some sample-test measurements were performed in order to achieve an acceptable figure of merit for the lowest possible energies. The figure of merit (M) [7] is defined as the ratio of the distance between the centroids of the ratio peaks to the sum of the FWHM of these peaks. We found that good separation of the neutron and gamma ratio peaks can be achieved by summing the first four samples of the integrated signal ($M > 1.5$). For an energy window set between 100 and 200 keV_{ee}, average pulse shapes corresponding to neutron and gamma interactions were recorded. Fig 3 shows the neutron and gamma integrated pulses normalized to the total charge (last sample).

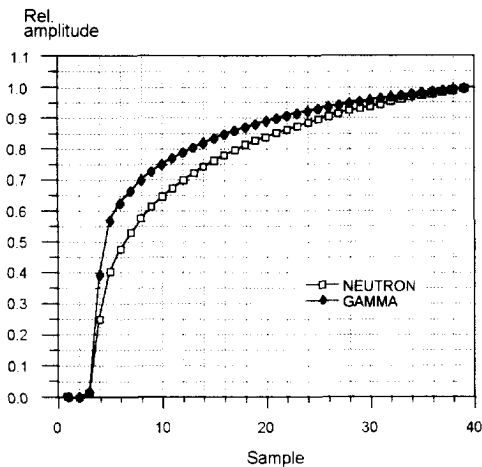


Fig. 3 Sampled signal at the gated integrator output. The signal is normalized to the total charge (last sample).

The optimal weights calculated as a function of the sample number are shown in Fig. 4. We approximated these weights by assigning non-zero values only to the samples number four and five. Note that the weighting function obtained is near optimal for our particular application (BC-501A liquid scintillator). In other applications, with different detector pulse shapes and longer decay time constants (e.g. inorganic scintillators), the outcome will generally be different. The use of a lower sampling frequency and a higher amplitude resolution of the ADC may then be a preferable choice.

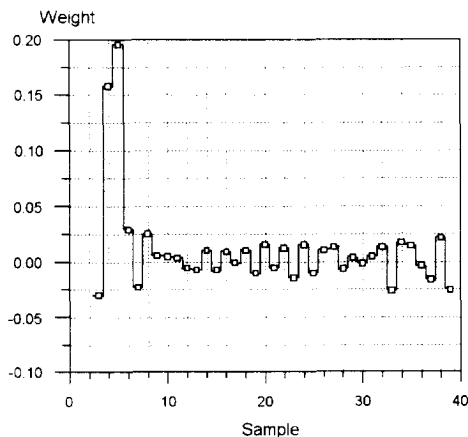


Fig. 4 Experimental weighting function.

The gated integrator integrates both the signal charge and the charge due to the dark current of the PMT. Thus, careful choice of the total integration time is important for achieving the ultimate performance from the pulse-shape analyzer. At short charge collection times the statistical uncertainties of the signal charge limits the performance of the analyzer while at long gating times the contribution of the dark current becomes noticeable. Therefore, there is an optimal duration of the total charge collection time. To estimate its value in our application, we recorded a series of ratio spectra for the

same energy interval (100 to 200 keV_{ee}) but for different integration times. From these data the optimal integration time was found to be 800 ns.

The discriminating ability of the processor as a function of the particle energies was also studied. Ratio spectra were recorded for different settings of the energy window and the figure of merit was calculated for each spectrum. Fig. 5 summarizes the results, showing that a good separation between gamma and neutron peaks is achieved for electron energies down to 30 keV_{ee}.

V. CONCLUSION

A digital pulse-shape analyzer was developed that allows a near-optimum separation algorithm to be used. The processor is simple and incorporates a single gated integrator followed by fast sampling ADC. Sampled data are corrected for the integrator pedestal and DC instabilities. A pileup rejection circuit is also incorporated. The performed measurements indicate a good neutron-gamma separation down to 30 keV electron equivalent energy.

VI. ACKNOWLEDGMENTS

We wish to thank David Stuenkel for his contribution during some of the measurements. The research was performed under the sponsorship of the U.S. Department of Energy Health Physics Research Award Program Administered by Oak Ridge Associated Universities under Management and Operating Contract DE-AC05-76OR0003.

VII. REFERENCES

- [1] F. D. Brooks, "A Scintillation Counter with Neutron and Gamma-Ray Discriminators", *Nucl. Instr. and Meth.*, Vol. 4, pp. 151-163, (1959).
- [2] J. M. Adams and G. White, "A Versatile Pulse Shape Discriminator for Charged Particle Separation and Its Application to Fast Neutron Time-of-Flight Spectroscopy". *Nucl. Instr. and Meth.*, Vol. 156, pp. 459-476, (1978).
- [3] B. Sabbah and A. Suhami, "An Accurate Pulse-Shape Discriminator for a Wide Range of Energies". *Nucl. Instr. and Meth.*, Vol. 58, pp. 102-110, (1968).
- [4] E. Gatti and F. De Martini, "A New Linear Method of Discrimination Between Elementary Particles In Scintillation Counters", *Nuclear Electronics 2*, IAEA Vienna, pp. 265-276, (1962).
- [5] F. De Martini and E. Gatti, "Optimum Linear Filter for Pulse Shape Recognition in the Presence of Thermal Noise". *Energia Nucleare*, Vol. 9, No. 3, March (1962).
- [6] R. Aleksan et al., "Pulse Shape Discrimination with a 100 MHz Flash ADC System". *Nucl. Instr. and Meth.*, Vol. A273, pp. 303-309, (1988).
- [7] R. A. Winyard, J. E. Lutkin and G. W. McBeth, "Pulse Shape Discrimination in Inorganic and Organic Scintillators. I". *Nucl. Instr. and Meth.*, Vol. 95, p. 141, (1972).

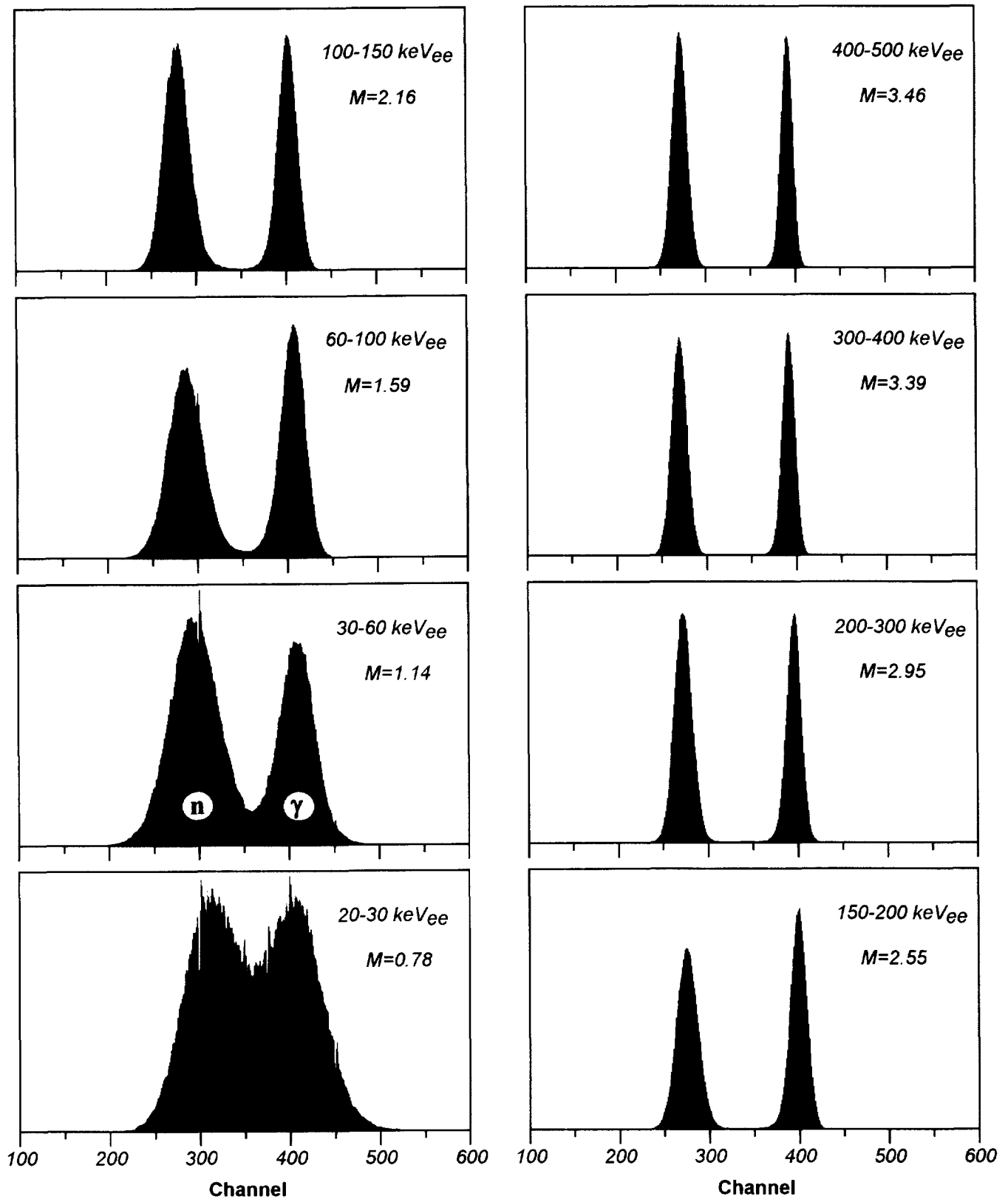


Fig. 5 Neutron-gamma ratio spectra for different energy windows.